Economic Dispatch by Secondary Distributed Control in Microgrids

Jacqueline Llanos[1 2], Juan Gomez[1], Doris Saez[1], Daniel Olivares[3] and John Simpson-Porco[4]
[1] University of Chile, Santiago, Chile.
[2] Universidad de las Fuerzas Armadas ESPE, Sangolquí, Ecuador.
[3] Pontificia Universidad Católica de Chile, Santiago, Chile.
[4] University of Waterloo, Waterloo, Canada
Email: jllanos@ug.uchile.cl, jdllanos@espe.edu.ec

Acknowledgments

This study was supported by FONDECYT Project 1170683, FONDECYT Project 1181517, the Complex Engineering Systems Institute (CONICYT/FB0816), the Solar Energy Research Center SERC-Chile (CONICYT/FONDAP/15110019) and Ph.D. scholarship from CONICYT Doctorado para Extranjeros/2015-21150555/2014-63140113.

Keywords

≪Smart microgrids≫, ≪Microgrid≫, ≪Energy system management≫, ≪Smart grids≫, ≪Distributed power≫, ≪Power management≫

Abstract

This paper proposes a distributed controller in order to achieve the economic dispatch (ED) of a microgrid, which complies with the Karush-Kuhn-Tucker optimality conditions for a linear optimal power flow formulation. The consensus over the Lagrange multipliers allows an optimal dispatch without considering an electrical microgrid model, preserving the frequency and voltage restoration into the secondary control level for isolated microgrids.

Introduction

With the increased penetration of Distributed Generation (DG) units based on renewable energy resources and distributed energy storage (DES) units, the microgrids have emerged as systems that allow the integration of these units. A microgrid is described as a cluster of DG units, DES units, and distributed loads, coordinated to supply electricity in order to fulfill economic, technical, and environmental requirements. The microgrids can operate in a grid-connected mode using a Point of Common Coupling (PCC) or in an isolated mode [1].

The microgrid, in general, assumes three critical functions: the control of the DG units, the energy management, and the protections of the microgrid [2]. A three level hierarchical control structure is used. The primary control maintain voltage and frequency stability, deviating the operation values when the power demanded changes, this level includes the inner control loops and droop control. The secondary control restores the frequency and the voltage to their nominal values, and the tertiary control achieves the optimal dispatch of the microgrid, and it manages the power flow between the microgrid and the main grid in grid-connected mode [1] [3] [4]. In the hierarchical architecture, the primary control is performed within a shorter time scale compared to the secondary control; while the optimal dispatch requires several minutes depending on the complexity of the optimization problem to be solved [5].

The existing secondary control strategies can be classified into three control approaches: centralized, decentralized, and distributed control. In the first approach, the central controller uses measurements from the whole microgrid to compensate the frequency and voltage deviations, however if the central controller fails the frequency/voltage restoration are not achieved.

The decentralized and distributed approaches are usually based on PI controllers in order to restore the frequency and the voltage [4] [7]. Decentralized approach uses just local measurements to achieve the regulation, whereas distributed approach uses information from neighbors DG units, requiring a communication network and increasing reliability and security in isolated microgrids [3] [6]. Nowadays a consensus algorithm is included to the distributed approach improving the real and reactive power sharing [5] [8].

The optimal operation is a tertiary control level task, and it is achieved by solving an economic dispatch problem. This controller is often formulated under a centralized approach, and requires several minutes to solve an optimization problem. However, in microgrids, the disturbances can be produced at seconds, then the optimal dispatch is not updated for this time scale. In order to solve the optimal dispatch at shorter times, it can be analyzed with decentralized or distributed control approaches.

The adaptive droop controller is a common technique used to achieve minimal operation cost based on decentralized schemes [9] and [10]. In this scheme, the DGs controllers are tuned according to its generation cost. However, due the DGs do not share information, the global minimum generation cost is not achieved in the microgrid.

Some techniques used for minimal cost based on distributed control approach are the following: incremental cost consensus estimated (ICC) [11], [12], and gradient consensus [13], [14]. The ICC is used in Multi-Agent System (MAS) [11], and it is based on consensus algorithm and incremental cost (IC). IC and global supply-demand mismatch are estimated for each generator [16], however, these works do not consider the generating power limits. In [11], [12], [17] external controllers are added in order to consider the power generating limits applying ICC approach, in these cases a pseudo generating cost for DG neighbors is estimated. Unlike ICC, the distributed gradient approach computes the incremental cost [13], [18]. All these works include the IC as the consensus variable.

Unlike the works above mentioned, our controller includes the Karush-Kuhn-Tucker (KKT) conditions from a centralized linear optimal power flow (OPF) formulation considering the generating power limits, using a distributed scheme. Our proposal is based on the distributed-averaging proportional-integral (DAPI) controller for frequency and voltage restoration proposed in [8]. We add an additional controller to the DAPI frequency loop to achieve the optimal economic dispatch of the microgrid. Notice that the design of this additional controller is a contribution itself. In order to the whole microgrid satisfy the KKT conditions, the DG units exchange information with their respective neighbors using a communication network.

The experimental results validate the adequate performance of the controller against sudden changes in the load and communication failures, the microgrid performance when a DG unit is disconnected is tested as well.

The contributions of this paper are as follow: i) the optimal dispatch and frequency restoration are considered in the same time scale in order to archive the optimal dispatch when fast disturbances occur, ii) the KKT optimality conditions of the linear centralized OPF problem are satisfied, iii) the microgrid topology is not required for achieve the optimal dispatch, iv) the proposed controller was tested in a experimental microgrid.

Economic Dispatch by Secondary Distributed Control in Microgrids

The design of the proposed distributed controller is based on a centralized optimal economic dispatch formulation and the KKT optimal conditions. A consensus algorithm over the Lagrange multipliers related to real power balance is considered as well. The proposed approach is described in detail below.

Average Consensus Algorithm

Consider the graph $G = (\mathcal{N}, \mathcal{E}, A)$, where $\mathcal{N} = \{1, .., n\}$ is the vertex set that represents the DG units in the microgrid, $\mathcal{E} \subset \mathcal{N} \times \mathcal{N}$ represents the edge set of communication links between DGs, and A is the $n \times n$ adjacency matrix of the graph. If DG $i \in \mathcal{N}$ exchanges information with DG $j \in \mathcal{N}$, then

$a_{ij} = a_{ji} = 1$, otherwise $a_{ij} = 0$. It is said that the consensus over variable x is achieved if $x_i(t) - x_j(t) \to 0$ for all vertices $i, j \in \mathcal{N}$. If G is connected, consensus is achieved via the first-order consensus algorithm $\dot{x}_i = -\sum_{j\in\mathcal{N}, j\neq i} a_{ij}(x_i - x_j)$; see [8].

Centralized Optimal Economic Dispatch

Prior to the distributed controller proposal design, a centralized optimal economic dispatch and its KKT optimality conditions are presented, which are used in the design of the controller proposed. We consider a balanced-load microgrid, with a set of DGs $\mathcal{N} = \{1, \ldots, n\}$, each one with a different operation cost defined as a function of its real power $C_i(P_i)$. In order to achieve the optimal economic dispatch a linear power flow formulation, based on a single-bus system, is designed as is shown in (1). The objective function (1a) is defined to minimize the operation cost of the microgrid; where $C_i(P_i)$ is a convex cost function defined by $C_i(P_i) = \mathrm{a}_i P_i^2 + \mathrm{b}_i P_i + \mathrm{c}_i$, P_i is the real power dispatched for the generator i, and a_i, b_i, and c_i, are the parameters function cost. The optimization problem is subject to power balance constraint by (1b), where P_D is the power demanded. The power limits of DGs constraint are defined in (1c).

$$
\begin{aligned}
&\text{minimize} && \textstyle\sum_{i\in\mathcal{N}} C_i(P_i) && && \text{(1a)}\\
&\text{subject to} && P_D = \textstyle\sum_{i\in\mathcal{N}} P_i && && \text{(1b)}\\
& && P_i^{\min} \leq P_i \leq P_i^{\max} && \forall\, i \in \mathcal{N} && \text{(1c)}
\end{aligned}
$$

The Lagrangian function of optimal dispatch problem (1) is shown in (2)

$$
\mathbb{L}(P_i, \lambda, \sigma_i^+, \sigma_i^-) = \sum_{i\in\mathcal{N}} C_i(P_i) + \lambda \left(P_D - \sum_{i\in\mathcal{N}} P_i \right) + \sum_{i\in\mathcal{N}} \sigma_i^+ (P_i - P_i^{\max}) + \sum_{i\in\mathcal{N}} \sigma_i^- (P_i^{\min} - P_i) \tag{2}
$$

Where λ represents the Lagrange multiplier associated to power balance constraint (1b), σ_i^- and σ_i^+ are the Lagrange multipliers associated to minimum and maximum power constraints (1c).

Notice that in the distributed proposal design, we consider the Lagrange multipliers σ_i^+ as the control action related to the maximum power limits of the DG unit, and Lagrange multipliers σ_i^- represents the control action related to the minimum power limits of the generating unit.

The KKT optimality conditions of the optimization problem (1) are defined as follow:

$$
\begin{aligned}
&\frac{\partial \mathbb{L}}{\partial P_i} = \nabla C_i(P_i) - \lambda + \sigma_i^+ - \sigma_i^- = 0 && i \in \mathcal{N} && \text{(3a)}\\
&\sigma_i^+ (P_i - P_i^{\max}) = 0 && i \in \mathcal{N} && \text{(3b)}\\
&\sigma_i^- (P_i^{\min} - P_i) = 0 && i \in \mathcal{N} && \text{(3c)}\\
&\sigma_i^+,\ \sigma_i^- \geq 0 && i \in \mathcal{N} && \text{(3d)}
\end{aligned}
$$

The primal feasibility conditions are defined by (1b) (1c).

Distributed Control Design

The proposed controllers have the following features: i) The secondary control and the optimal economic dispatch are solved in the same time scale, ii) The distributed control approach is used, iii) The optimal dispatch is achieved using PI controllers, iv) The real-time measurements are used in order to obtain the economic optimal dispatch, v) The control actions for frequency regulation and optimal dispatch are added to the droop controller, vi) The communication network is connected, bidirectional and ideal (without large time-delays). vii) The communication topology is different from the electrical network topology.

Secondary control and the optimal economic dispatch need to be solved in the same time scale. The first stage comprises the design of secondary control for frequency and voltage restoration, then in the second stage a new term is added in order to achieve the economic dispatch.

Distributed Secondary Control

The frequency restoration is achieved using the DAPI controller proposed in [8], it is shown in (4)–(5) , where m_i is $P-\omega$ droop coefficient, P_i is the real power injection, ω^* is the nominal frequency and ω_i corresponds to frequency regulated in the ith DG. The DAPI control action Ω_i is obtained from (5), where the terms a_{ij} are the entries of the adjacency matrix; thus, the control action Ω_j is shared with generator i only if a_{ij} is nonzero.

$$\omega_i = \omega^* - m_i P_i + \Omega_i \tag{4}$$
$$k_i \dot{\Omega}_i = -(\omega_i - \omega^*) - \sum_{j\in\mathcal{N},j\neq i} a_{ij}(\Omega_i - \Omega_j) \tag{5}$$

Also, DAPI voltage-regulation and reactive-power-sharing controllers are implemented based on [8]. The control law of this controller is represented by equations (6) and (7), where e_i is the control action for voltage regulation, E_i is the voltage of the ith DG, n_i represents the Q-E droop coefficient, E^* is the microgrid nominal voltage, Q_i^* is the reactive power rating of unit i, β_i and k_i are positive gains, and a_{ij} is an element of the adjacency matrix of communication between DGs. In this case e_i establishes a trade-off between voltage regulation and reactive power sharing.

$$E_i = E^* - n_i Q_i + e_i \tag{6}$$
$$\mathbf{k_i} \dot{e}_i = -\beta_i (E_i - E^*) - b_i \sum_{j\in\mathcal{N},,j\neq i} a_{ij} \left(\frac{Q_i}{Q_i^*} - \frac{Q_j}{Q_j^*} \right) \tag{7}$$

Distributed Secondary and Economic Dispatch Control

In order to achieve the optimal economic dispatch the droop frequency ω_i in (4) is modified. As is shown in (8) the term ρ_i is added, and its design is based on the centralized optimal economic dispatch (1).

$$\omega_i = \omega^* - m_i(P_i) + \Omega_i + \rho_i \tag{8}$$

We include the first KKT optimality condition (3a) in the proposed controller obtaining the λ_i multiplier as is shown in (9).

$$\lambda_i = \nabla C_i(P_i) + \sigma_i^+ - \sigma_i^- \tag{9}$$

Notice that λ_i is related to the power balance in the microgrid and it should be equal to λ multiplier on (3a) in order to achieve a global balance. Then in the distributed scheme, a consensus algorithm over whole λ_i multipliers is defined in (10), where ρ_i is considered as the consensus control action.

$$k_i^1 \dot{\rho}_i = -\sum_{j\in\mathcal{N},j\neq i} a_{ij}(\lambda_i - \lambda_j) \tag{10}$$

The Lagrange multipliers from the centralized optimal economic dispatch are represented as control actions in the proposed distributed controllers. In this context the σ_i^+ distributed controller shown in (11) is designed to ensure the operation below the maximum limit of real power generation. This controller is activated if the active power in the DG_i is greater than its maximum limit, and the term $k_i^3\sigma_i^+$ is added in order to guarantee that $\sigma_i^+ = 0$, achieving the same performance of the multipliers in the centralized problem, if this constraint is not activated. σ_i^- distributed controller shown in (12) is designed to ensure the operation over the minimum limits of real power generation in all DG units, this controller is designed in the same way than σ_i^+ controller.

$$k_i^2 \dot{\sigma}_i^+ = \mu_i^2 \max\left\{ P_i + \frac{1}{\mu_i^2} k_i^3 \sigma_i^+ - P_i^{\max}, 0 \right\} - k_i^3 \sigma_i^+ \tag{11}$$

$$k_i^4 \dot{\sigma}_i^- = \mu_i^3 \max\left\{ P_i^{\min} + \frac{1}{\mu_i^3} k_i^5 \sigma_i^- - P_i, 0 \right\} - k_i^5 \sigma_i^- \tag{12}$$

The stationarity centralized KKT condition (3a) is satisfied through (9) in the distributed controller, the complementary slackness constraints (3b) and (3c) are satisfied by (11) and (12) respectively. The dual feasibility contraints (3d) are satisfied by (11) and (12). Finally the primal feasibility condition defined by (1b) is satisfied by (5), and the primal feasibility condition defined by (1c) is satisfied by (11) and (12).

Distributed Secondary and Economic Dispatch Control Scheme

Fig. 1 shows the architecture of the local controller implemented in each DG that enables the distributed control strategy. The first layer corresponds to voltage and current control, also a virtual impedance is added for microgrids with resistive lines [15]. The second layer correspond to primary control droop, where the terms of the equations (8) and (6) are calculated using local measurements. The equation (6) and (8) are modified by the third control layer. This layer includes the distributed controllers for frequency and voltage restoration and economic dispatch. We added the term Ω_i from (5) in order to achieve frequency restoration, and ρ_i in order to achieve the economic dispatch of the microgrid, this is obtained from (9), (10), (11) and (12).

The proposed controller receives from each neighbor j the following information: Ω_j, λ_j, Q_j and Q_j^*, while it sends Ω_i, λ_i, Q_i and Q_i^*. The exchange of information between local DG controllers occurs through the communication network.

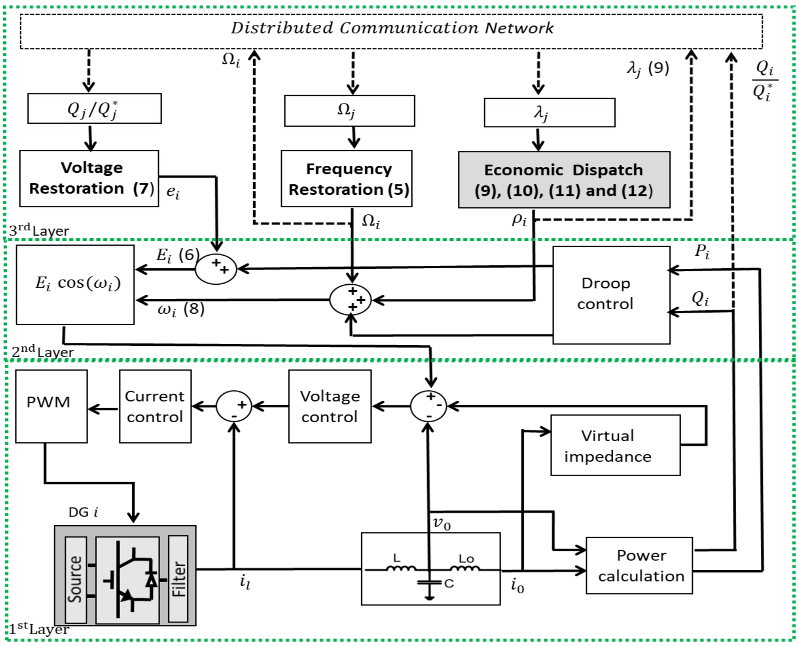

Fig. 1: Distributed control scheme

Experimental Results

In order to validate the proposed controllers, experimental tests were performed in the Laboratory of Microgrids Control at the University of Chile shown in Fig. 2. The microgrid topology is composed of three converters, two local loads and two power lines. The characteristics of DG units and network parameters are given in Table I and Table II, respectively. Ethernet communication network is implemented to share information among DGs, as is shown at left side of Fig. 2, and it is able to emulate a communication failure. The topologies, as well as the adjacency matrix A, with and without failure, are shown in Fig. 3.

In this work different operating costs of each DG are considered, DG 2 has the lowest operating cost and DG 3 is the more expensive, the generating cost function (13) of each DG unit is assumed quadratic, the

Table I: DG characteristics

Parameter	Symbol	DG1-DG3
Max Active Power	P_i^{max}	2kW
Min Active Power	P_i^{min}	0kW
P-W Droop Coefficient	m_i	$2.5\cdot 10^{-3}\,\frac{\text{rad}}{\text{W}\cdot\text{s}}$
Q-E Droop Coefficient	n_i	$1.5\cdot 10^{-3}\,\frac{\text{V}}{\text{var}}$
Frequency Control Gain	k_i	0.5s
Voltage Control Gain	$\mathbf{k_i}$	1s
OD Control Gain	k_i^1	0.5s
Max Power Control Gain	k_i^2	0.1s
Min Power Control Gain	k_i^4	0.1s
Return to Zero Gain	$\frac{k_i^3}{u_i^2}, \frac{k_i^5}{u_i^3}$	0.01s

Table II: Microgrid parameters

Parameter	Symbol	Value
Nominal Frequency	$\omega^*/2\pi$	50 Hz
Nominal Voltage	E^*	150 V
Filter Capacitance	C	25μF
Filter Inductance	L_f	1.8mH
Coupling Inductance	L_o	2.5mH
Sampling Period	T_{SP}	1/16E3 S
Load 1	L_1	11Ω
Load 2	L_2	22Ω
Line Impedance	L_ij	2.5mH
Cutoff f−Droop filter	ω_c	1*2π rad/S

parameters used in this work are shown in Table III.

$$C_i(P_i) = \mathrm{a}_i P_i^2 + \mathrm{b}_i P_i + \mathrm{c}_i \tag{13}$$

Three operating scenarios are evaluated. i) Load impacts scenario. ii) Communication links failures scenario, where a failure of the communication link between DG 1 and DG 3 is produced (See Fig. 3b). iii) Controller performance when the DG 3 is disconnected of the microgrid.

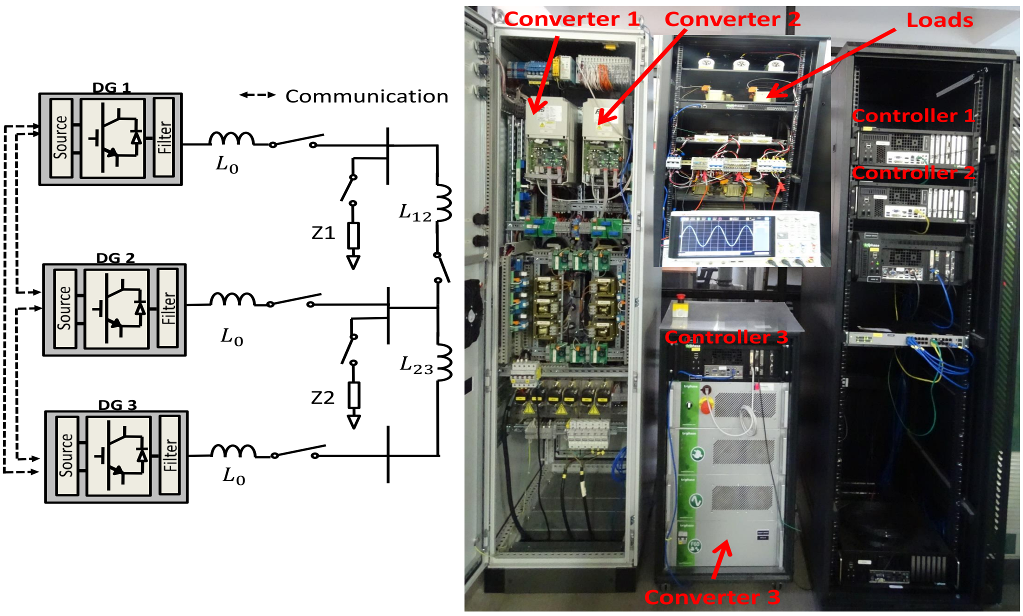

Fig. 2: Microgrid experimental setup

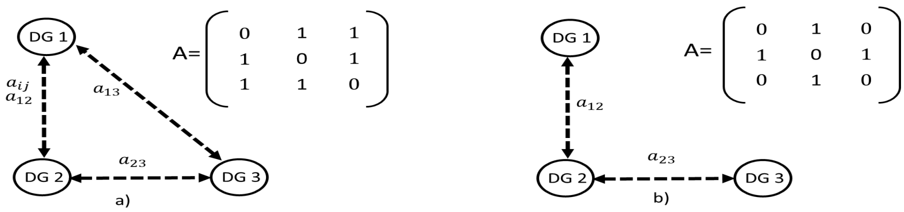

Fig. 3: Microgrid communication topology a) Original topology b) Topology with communication links failure

Table III: DG Cost parameters

Parameter	DG1	DG2	DG3
a_i [$\$/kW^2$]	0.444	0.264	0.5
b_i [$\$/kW$]	0.111	0.067	0.125
c_i [\$]	0	0	0

Distributed Controller Performance

Fig. 4 and Fig. 5 show the experimental results when the load changes. At time-frame 1, the load 1 and the distributed control for frequency and voltage restoration are activated (equations (5) and (7)). At time-frame 2, the distributed proposed controller for economic dispatch is also activated (equations (9), (10), (11) and (12)). At time-frame 3 the load 2 is added, finally at time-frame 4 the load 2 is removed.

As it can be seen in Fig. 4a the frequency remains in the nominal value, when the proposed controller is activated (time-frame 2-4) and also when the load changes occurs (time-frame 3 and 4). Fig. 4b shows the voltage at the output of the three converters, as it can be seen the voltage remains in the nominal value in steady-state.

Fig. 5 shows the real power generated by each DG unit, at time-frame 1 the real power is sharing by the units because only the frequency and voltage restorators are activated, also the power injected to the microgrid is equal in all DG units because their characteristics are the same. At time-frame 1 and 2 the load does not change, as it can be seen at time-frame 2 the DG units are re-dispatched considering the operating cost of each unit in order to archive the economic dispatch of the microgrid, the DG 2 generates more real power than the other units because its operating cost is the lowest, while DG 3 injects less real power than the other DG units because this is more expensive. The good performance of the proposed controller is shown with an increment and decrement of load at time-frame 3 and time-frame 4 respectively.

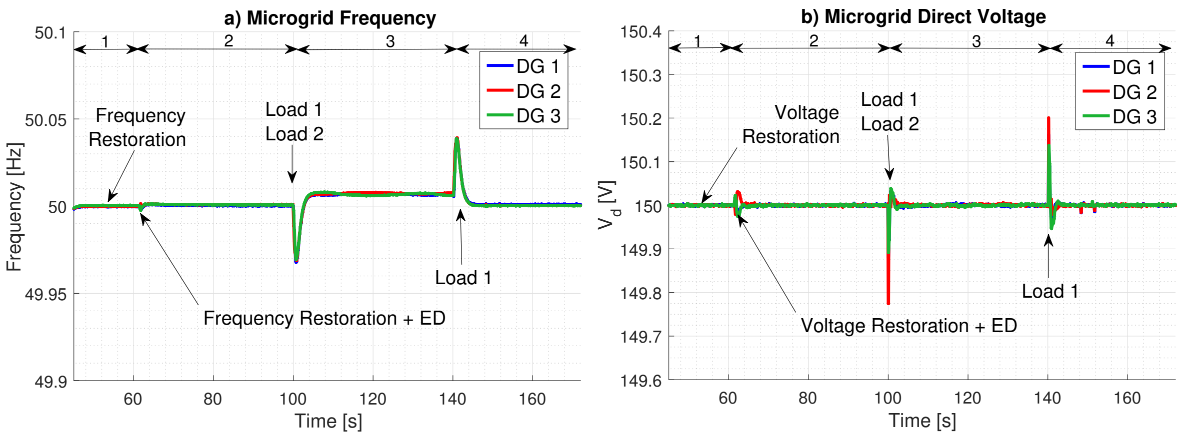

Fig. 4: Distributed control response a) Frequency b) Voltage

Fig. 6 shows the total operating cost of the microgrid at the time-frame under study. The analysis includes two approaches. The blue line shows the total cost for the proposed distributed controller. The red line shows the total operating cost obtained from an optimal centralized dispatch performed off-line for each operating point, this approach might be on-line solved, however, a high computationally burden is involved. As it can be see the total cost of our proposal is the same as the total cost obtained by optimal centralized dispatch approach. Our proposal solves the optimal economic dispatch using PI controllers and achieves the same results obtained by the centralized approach. It is worth mentioning that the centralized optimal dispatch was performed off-line for the three operation points shown in Fig. 6 with the aim to evaluate the economic performance of our proposal.

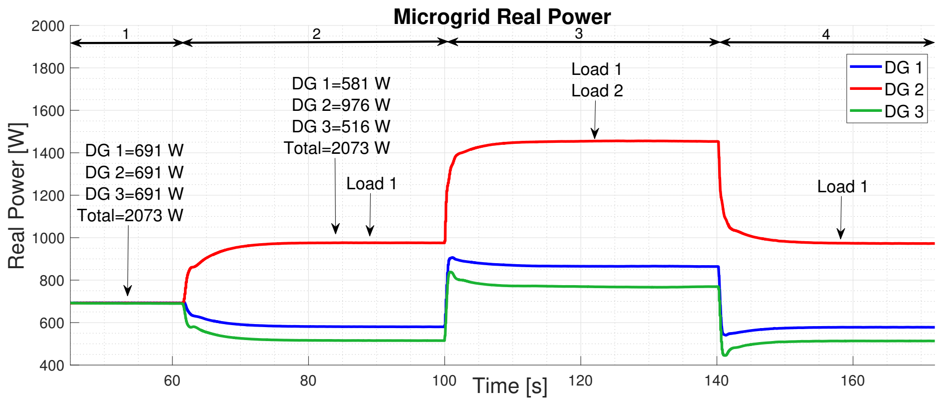

Fig. 5: Distributed control response - Real Power

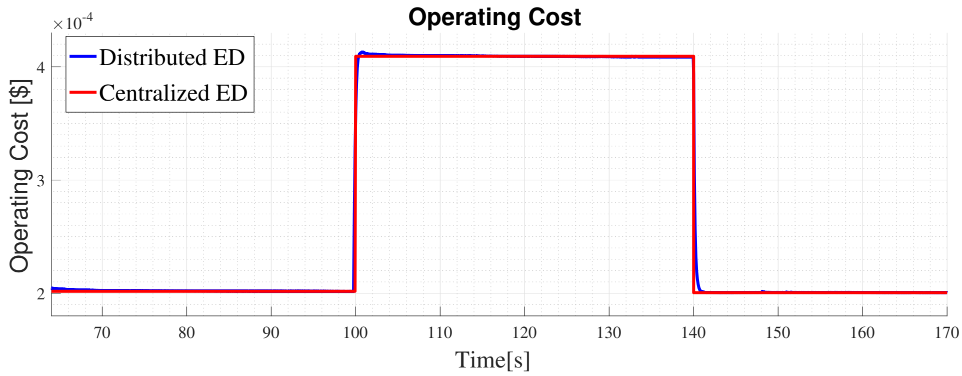

Fig. 6: Operating cost

Communication link failure

Fig. 7 and Fig. 8 show the performance of the proposed distributed controller when a communication link failure occurs. At time-frame 1, load 1, and all controller proposed (frequency and voltage restoration and economic dispatch) are activated, at time-frame 2 the communication link between DG 1 and DG 2 fails (Fig. 3b). Finally at time-frame 3 an incremental of load is produced (load 1 and load 2). As it can be seen the frequency (Fig. 7a) and voltage (Fig. 7b) remain in the nominal value when the communication link failure is produced.

In Fig. 8, the real power does not change when a communication link failure is produced (time-frame 2), because the controller detects the change in the communication network topology through the adjacency matrix, which is included in the consensus algorithm of the controller. Notice that the communication network topology is connected when the fail is produced.

Disconnection of a DG unit

In this scenario the DG 3 is disconnected, the results are shown in Fig. 9 and Fig. 10. During the time-frame 1 the proposed controllers (frequency and voltage restoration and economic dispatch) are activated, at time-frame 2 the DG 3 is disconnected, finally at time-frame 3 the load is increased.

In Fig. 9a and Fig. 9b the frequency and voltage are restored respectively to the nominal value when the disconnection of DG 3 is produced (time-frame 2 and time-frame 3). Fig. 10 shows the results of the real power injected, at time-frame 2 when the DG 3 is disconnected the real power is re-dispatched considering the operating cost of each DG, thus the DG 2 supplies more real power than DG 1 because the operating cost of DG 2 unit is lower. In order to validate the controller performance when a DG unit is disconnected an incremental load is produced (time-frame 3). As it can be seen the frequency and voltage are restored to their nominal values, at the same time the operating cost of DG units are considered.

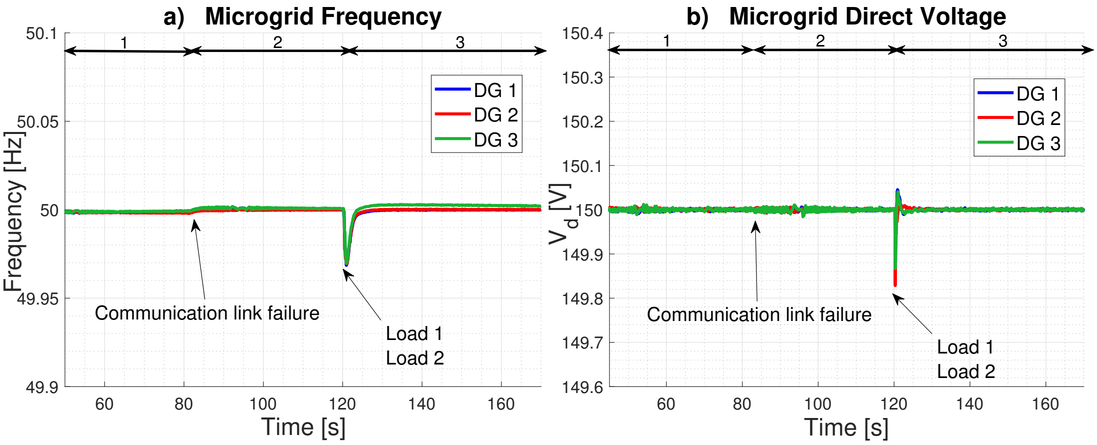

Fig. 7: Distributed control response test by communication link failure a) Frequency b) Voltage

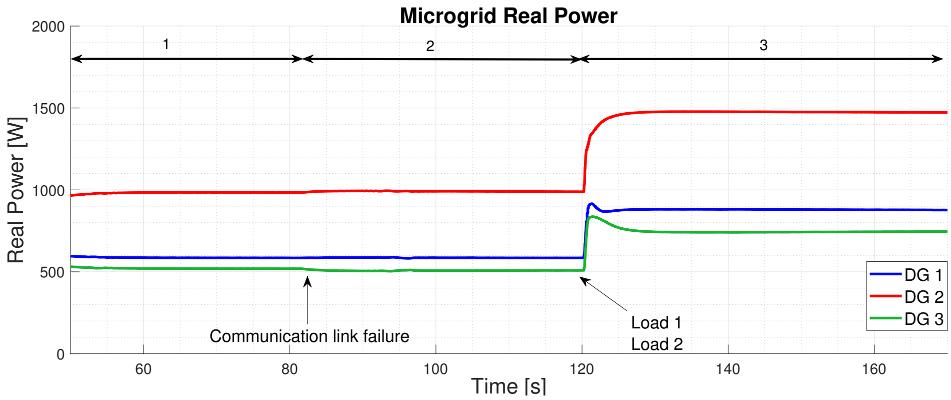

Fig. 8: Distributed control response test by communication link failure - Real Power

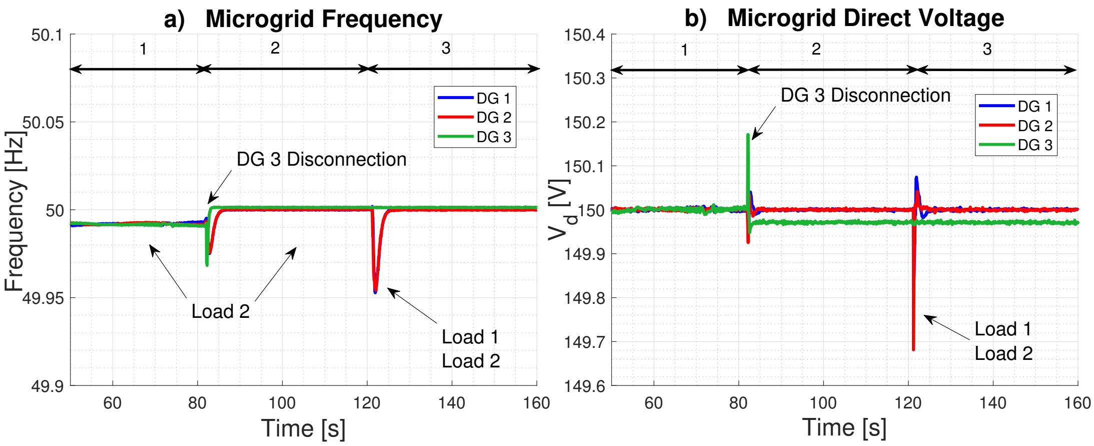

Fig. 9: Distributed control response test by disconnecting DG3 a) Frequency b) Voltage

Conclusion

The experimental results validate the good performance of the distributed controller proposed against sudden changes in the load, failures in the communications links as well as plug-and-play operation of DG units. The distributed controller proposed achieves the minimum operating cost at the same time that the frequency and voltage are restored. The controller of each DG uses its local measurements and information exchanged among neighboring DG units through a communication network. In order to address economic dispatch, the controller includes the first KKT condition in the formulation, and it does not need to know the topology of the microgrid.

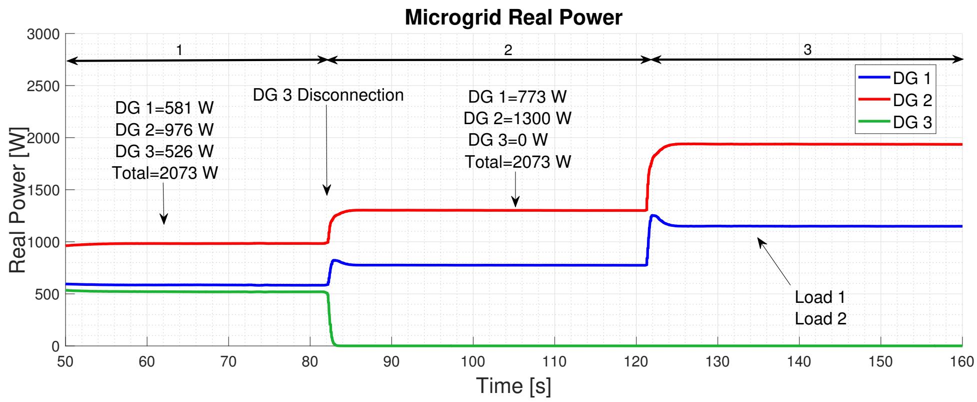

Fig. 10: Distributed control response test by disconnecting DG3 - Real Power

References

[1] Olivares D.E., Mehrizi-Sani A., Etemadi A. H. and Caizares C., "Trends in microgrid control", IEEE Transactions on Smart Grid., Vol 5, no 4, pp. 1905- 1919, 2014.

[2] Katiraei F., Iravani R., Hatziargyriou N., and Dimeas A., "Microgrids management", IEEE power and energy magazine, Vol 6, no 3, pp. 54-65, 2008.

[3] Bidram A., and Davoudi A., "Hierarchical structure of microgrids control system", IEEE Transactions on Smart Grid, Vol 3, no 4, pp. 1963-1976, 2012.

[4] Guerrero J.,Vasquez J, Matas J., Garcia L., Castilla M., "Hierarchical control of droop-controlled AC and DC microgridsA general approach toward standardization", IEEE Transactions on Industrial Electronics, Vol 58, no 1, pp. 1158-172, 2011.

[5] Feng X.,Shekhar A., Yang F., Hebner R., and Bauer P., "Comparison of hierarchical control and distributed control for microgrid", Electric Power Components and Systems, Vol 55, no 10, pp. 1043-1056, 2017.

[6] Yazdanian M., and Mehrizi-Sani A., "Distributed control techniques in microgrids", IEEE Transactions on Smart Grid, Vol 5, no 6, pp. 2901-2909, 2014.

[7] Shafiee Q., Guerrero J., and Vasquez J., "Distributed secondary control for islanded microgrids A novel approach", IEEE Transactions on Power Electronics,Vol 29, no 2, pp. 1018-1031, 2014.

[8] Simpson-Porco J., Shafiee Q., Dorfler F., Vasquez J., Guerrero J., and Bullo F., "Secondary Frequency and Voltage Control of Islanded Microgrids via Distributed Averaging", IEEE Transaction Industrial Electronics, Vol 62, no 11, pp. 1430-1441, 2015.

[9] Nutkani I. U., Loh P. C., and Blaabjerg F., "Autonomous Droop Scheme With Reduced Generation Cost, IEEE Transaction Industrial Electronics, Vol 61, no 12, pp. 6803-6811, 2014.

[10] Nutkani I. U., Loh P. C., and Blaabjerg F., " Cost-prioritized droop schemes for autonomous AC microgrids", IEEE Trans. Power Electron., Vol. 30, no. 2, pp. 11091119, 2015.

[11] Li C., Savaghebi M., J.C. Vasquez, and Guerrero J.M., "Multiagent based distributed control for operation cost minimization of droop controlled AC microgrid using incremental cost consensus, 2015 17th Eur. Conf. Power Electron. Appl. EPE-ECCE Eur, 2015.

[12] Li C., Vasquez J.C., and Guerrero J.M., "Convergence Analysis of Distributed Control for Operation Cost Minimization of Droop Controlled DC Microgrid Based on Multiagent, in 2016 IEEE Applied Power Electronics Conference and Exposition (APEC),pp. 3459 3464, 2016.

[13] Chen G. and Feng E., "Distributed secondary control and optimal power sharing in microgrids, IEEE/CAA J. Autom. Sin., Vol. 2, no. 3, pp. 304 312, 2015.

[14] Chen G. and Zhao Z., "Distributed optimal active power control in microgrid with communication delays, in Chinese Control Conference, CCC, pp. 7515 7520, 2016.

[15] Micallef A., Apap M., Spiteri-Staines C. and Guerrero J. and Vasquez J., "Reactive power sharing and voltage harmonic distortion compensation of droop controlled single phase islanded microgrids, IEEE Transactions on Smart Grid, Vol. 5, no. 3, pp. 1149–1158, 2014.

[16] Gang C., Ren J. and Feng N. E., "Distributed Finite-Time Economic Dispatch of a Network of Energy Resources, IEEE Transactions on Smart Grid, Vol. 8, no. 2, pp. 822-832, 2017.

[17] Chengcheng Z., Jianping H.,Peng C. and Jiming C., ., "Consensus-based energy management in smart grid with transmission losses and directed communication, IEEE Transactions on Smart Grid, Vol. 8, no. 5, pp. 20492061, 2017.

[18] Chen G. and Guo Z., "Distributed Secondary and Optimal Active Power Sharing Control for Islanded Microgrids With Communication Delays, IEEE Transactions on Smart Grid, Vol. 10, no. 2, pp. 2002-2014, 2019.